Supplementary Information

Emergence of Metallicity in Silver Clusters in the 150 Atom Regime: A Study of Differently Sized Silver Clusters

Indranath Chakraborty, Jayanthi Erusappan, Anuradha Govindarajan, K. S. Sugi, Thumu Udayabhaskararao, Atanu Ghosh and Thalappil Pradeep*

**DST Unit of Nanoscience (DST UNS), Department of Chemistry, Indian Institute of Technology Madras, Chennai 600 036, India; Fax: 91-44-2257 0545;*

E-mail: pradeep@iitm.ac.in

Supporting information

Method of Jacobian correction

To amplify the less-intense absorption features at the red end of the spectrum, the data have been corrected with the Jacobian factor. For this, the experimentally obtained absorbance values as a function of wavelength [I(ω)], were converted to energy-dependent numbers [I(E)], using the expression,

$$\mathbf{I(E) = \frac{I(\omega)}{\partial E/\partial \omega} \propto I(\omega)^* \omega^2}$$

Where ∂E/∂ω represents the Jacobian factor.

S1. Supporting information 1

Laser dependency of Ag_{152} cluster

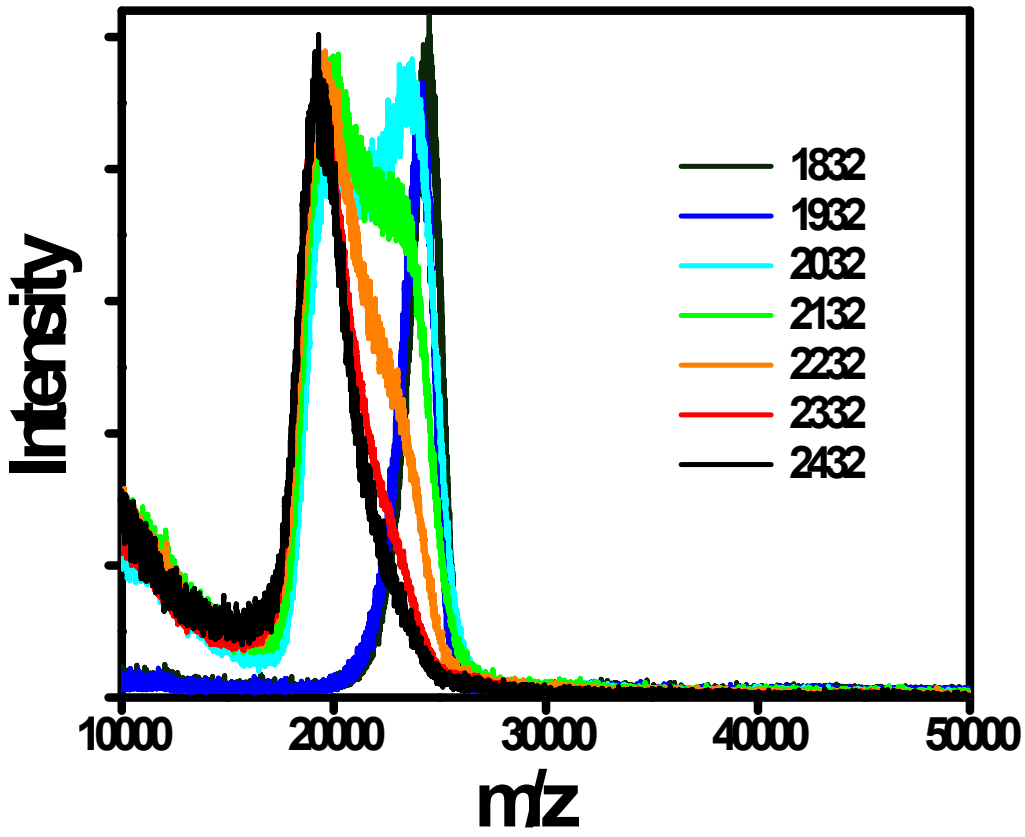

Fig.S1. Laser intensity dependent mass spectrum of Ag_{152} cluster. With increase (by 1000 units) in laser intensity from 1832 to 2432 (numbers refer to instrument settings and not absolute value of laser power), the peak shifts to lower values of m/z. Further increase in laser intensity does not change the peak position.

S2. Supporting information 2

Comparative mass spectra clusters

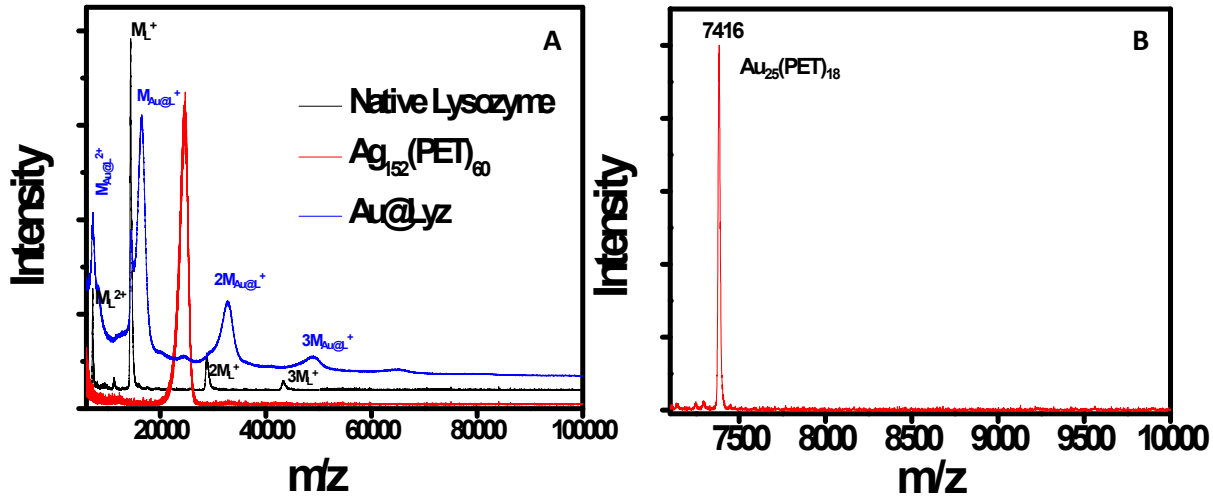

Fig.S2. A: Comparison of the mass spectra of PET protected silver cluster [$Ag_{152}(PET)_{60}$], native lysozyme (Lyz) and lysozyme-gold cluster (Au@Lyz). M_L^+ refers to the molecular ion on Lysozyme. The peak shift in Au@Lyz peak position is due to the Au cluster nucleated within the protein. $2M_L^+$, $3M_L^+$,… are dimer, trimer, etc. of the protein and the corresponding clusters. ML also shows a dication (M_L^{2+}) feature. B: MALDI MS data of $Au_{25}PET_{18}$

S3. Supporting information 3

Comparative MALDI MS of Ag_{152} and Ag_{44} clusters

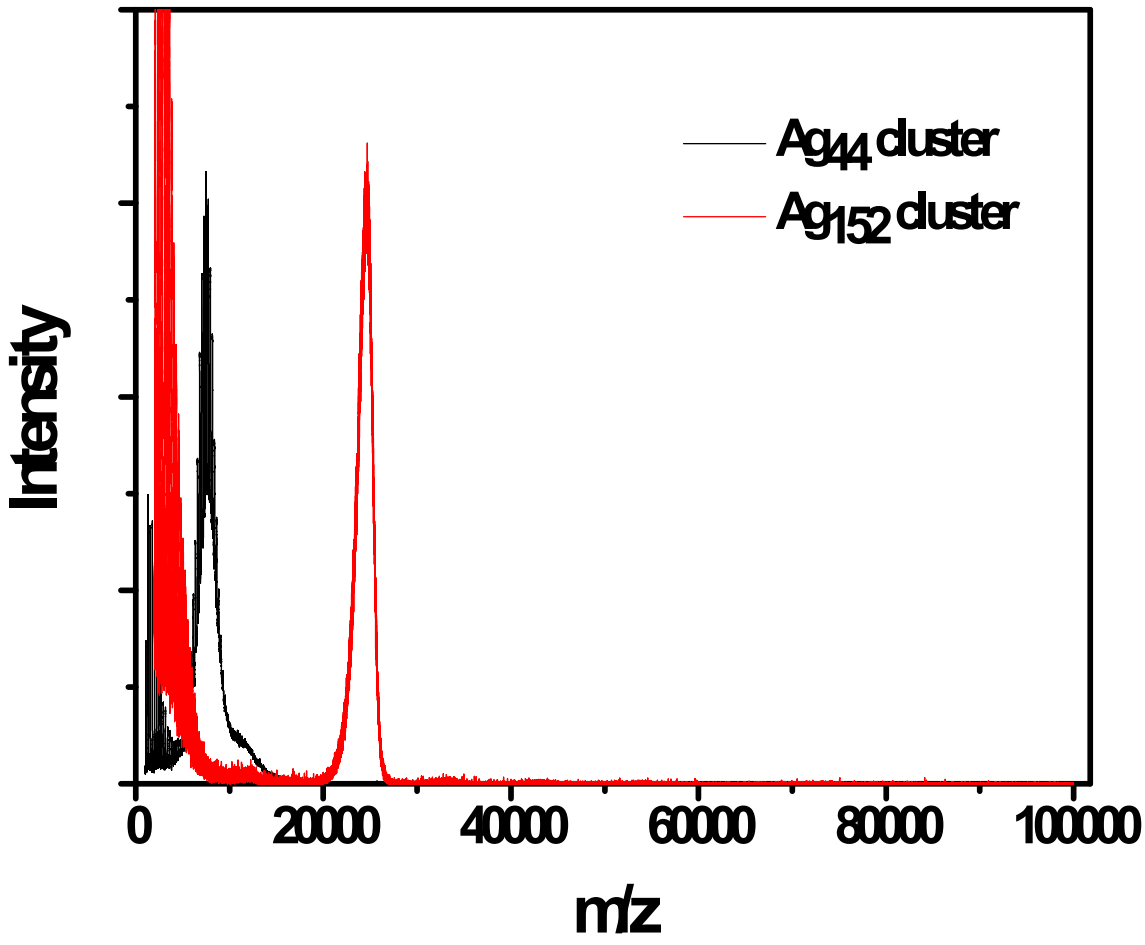

Fig. S3. MALDI MS spectra of Ag_{44} and Ag_{152} clusters using DCTB as a matrix.

S4. Supporting information 4

SEM/EDAX of ~Ag_{202} cluster

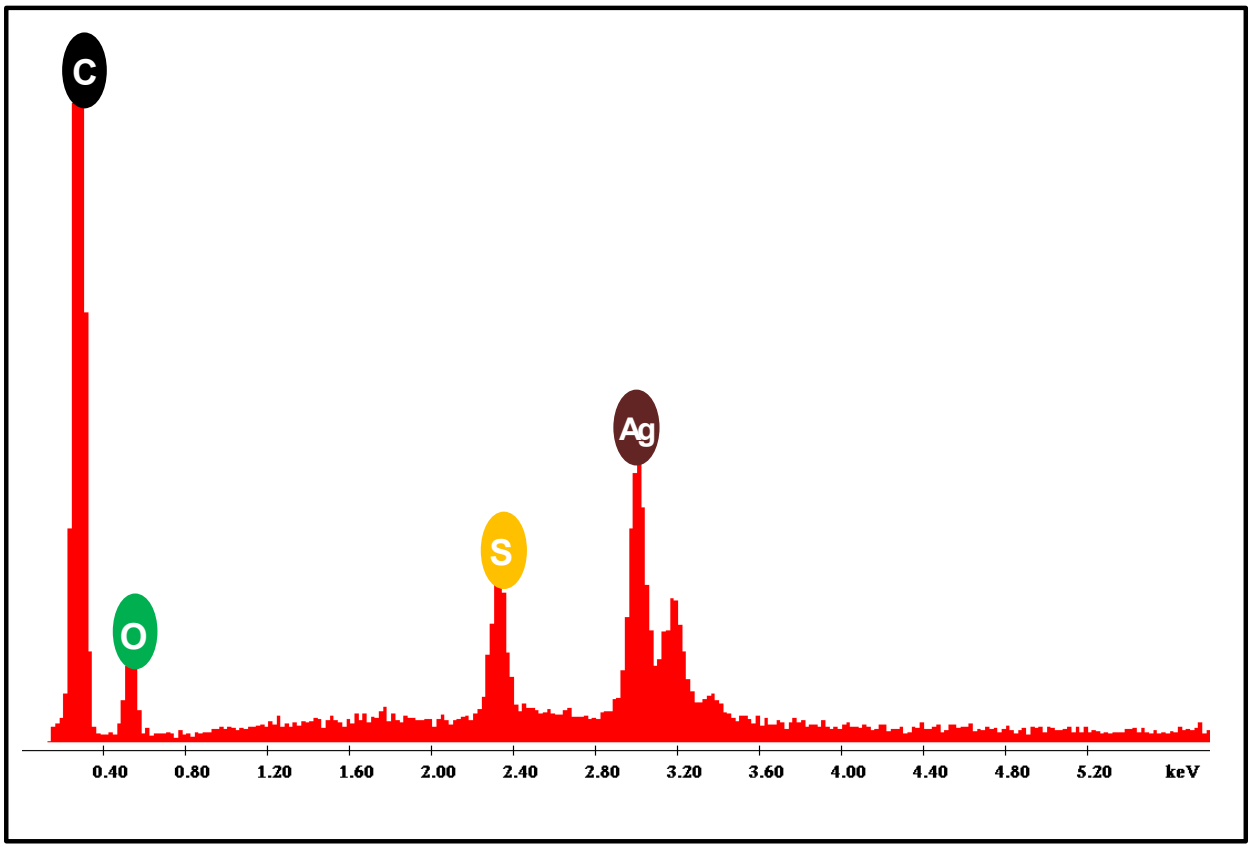

Fig.S4. SEM/EDAX of ~Ag_{202} cluster. The spectrum was collected from the solid sample spotted on a carbon tape. Absence of sodium shows the purity of the cluster.

S5. Supporting information 5

TEM image of ~Ag_{530} cluster

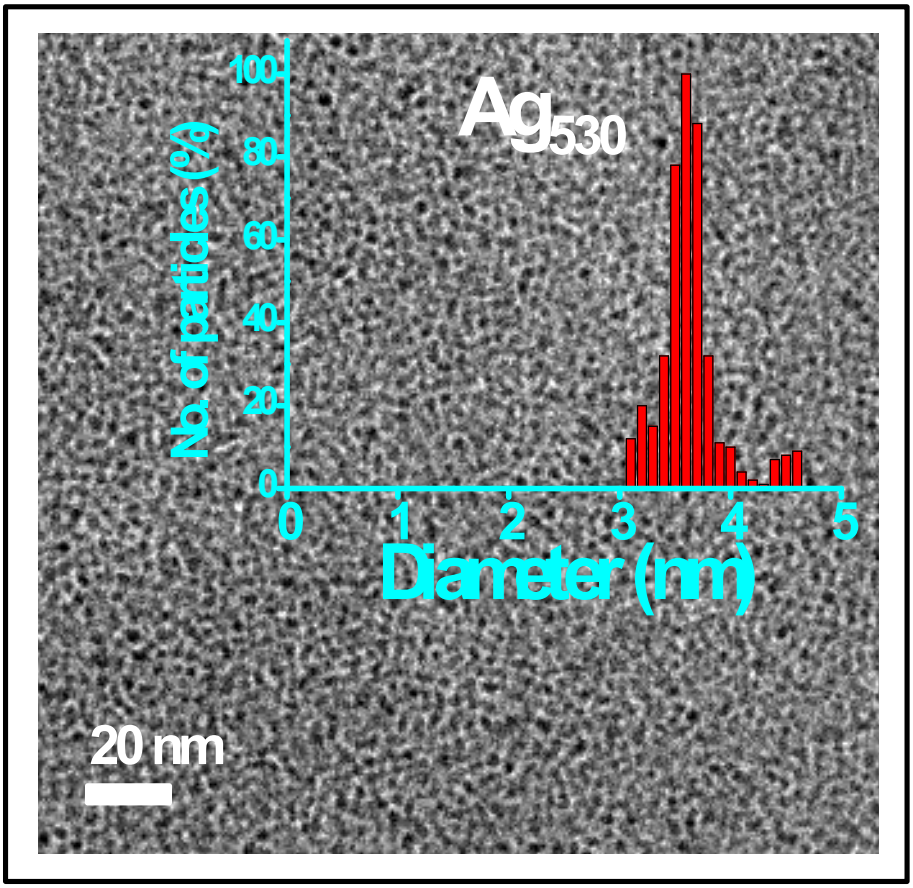

Fig.S5. TEM image of ~Ag_{530} cluster showing nearly homogeneous particles. Inset shows the size distribution of clusters ranging from 3 to 4 nm with an average diameter of 3.61 nm. The image also shows particles of a few different sizes, in agreement with the mass spectrum (Fig.1, main text).

S6. Supporting information 6

DLS of PET protected clusters

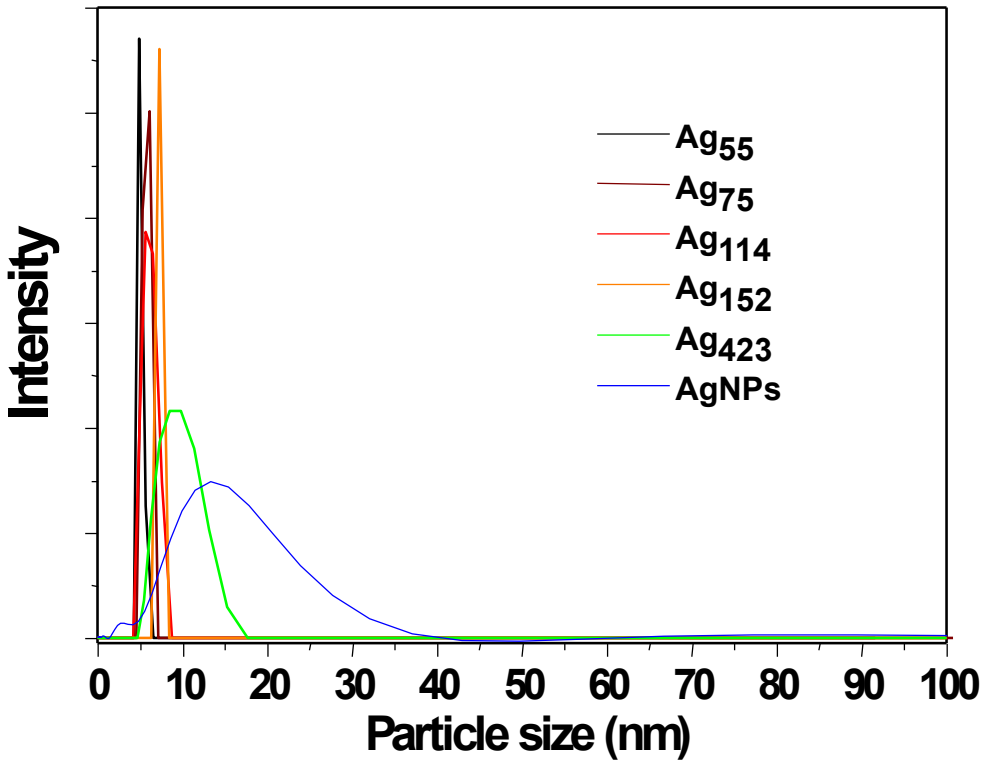

Fig.S6. DLS spectra of different sized PET protected silver clusters.

S7. Supporting information 7

MALDI MS and TEM of Ag@PET NPs

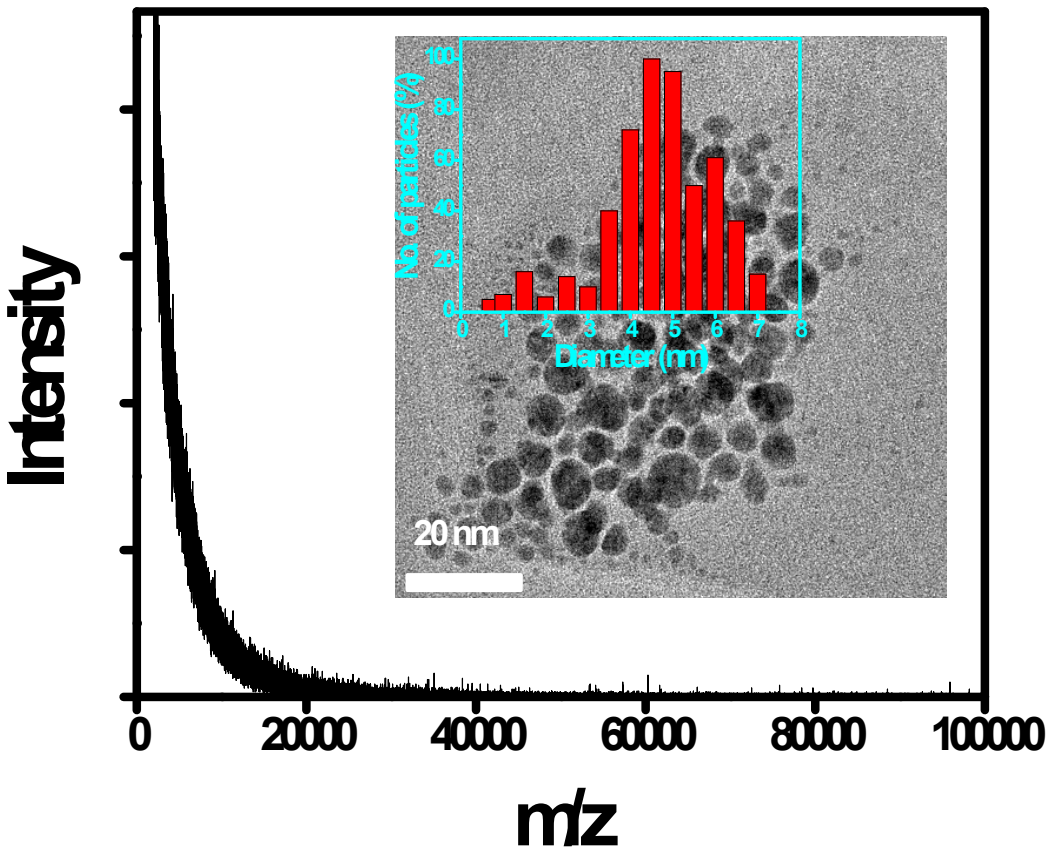

Fig.S7. The MALDI MS of Ag@PET nanoparticles which does not exhibit any distinct feature. Inset shows the corresponding TEM images which shows various sizes. Inset of inset shows the size distribution with an average diameter of 4.8 nm. In a typical synthesis, Ag nanoparticles are polydisperse.

S8. Supporting information 8

Absorption spectra of clusters in terms of energy

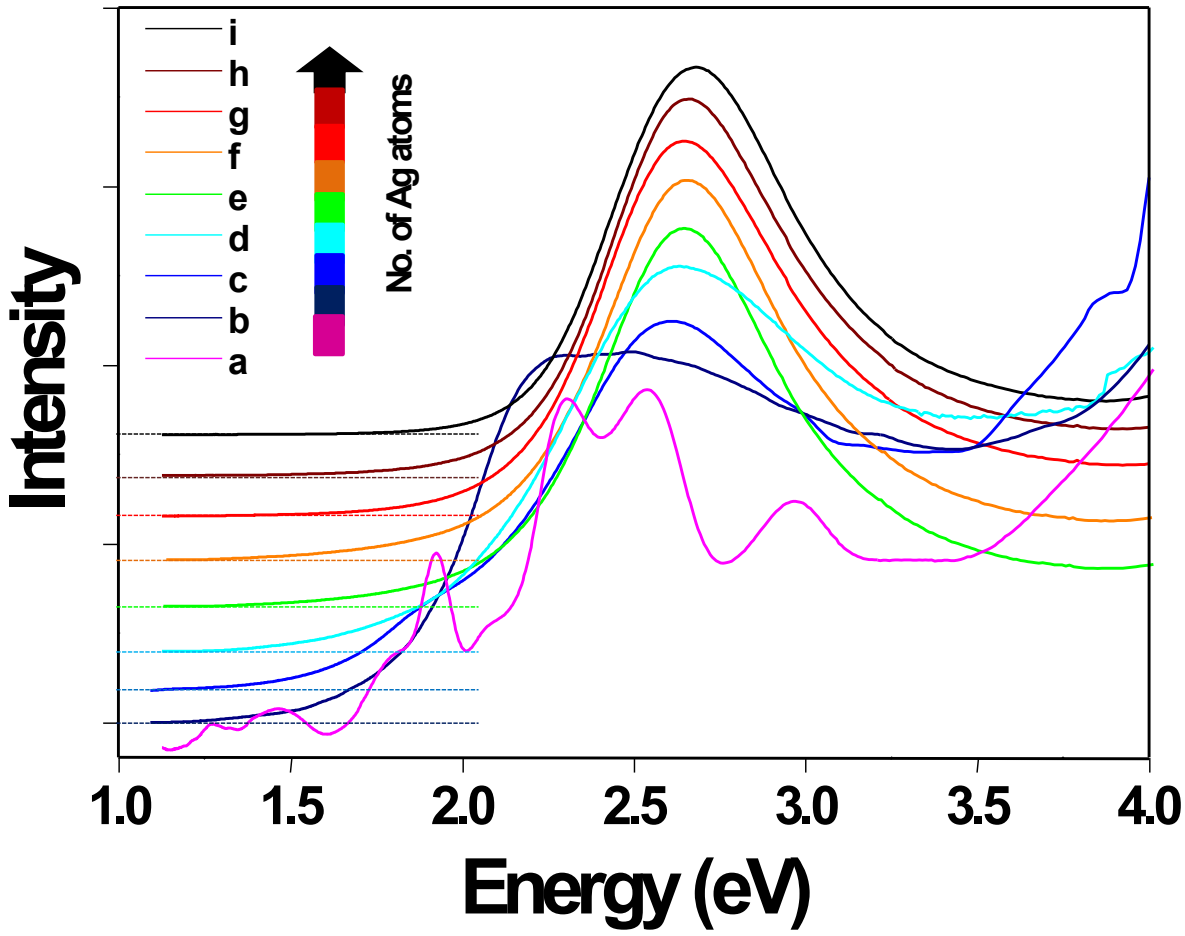

Fig.S8. Absorption spectra of clusters plotted in terms of energy, after normalization. The spectra correspond to (from bottom to up) Ag_{44} [a], Ag_{55} [b], ~Ag_{75} [c], ~Ag_{114} [d], Ag_{152} [e], ~Ag_{202} [f], ~Ag_{423} [g], ~Ag_{530} [h] and AgNPs [i].